Journal of Magnetic Resonance 201 (2009) 1–6

Contents lists available at ScienceDirect

Journal of Magnetic Resonance

journal homepage: www.elsevier.com/locate/jmr

A method for improved quantification of ^{1}H NMR signals under low-resolution conditions for solids

Yamini S. Avadhut [a], Denis Schneider [b], Jörn Schmedt auf der Günne [a,*]

[a] Department Chemie und Biochemie, Ludwig-Maximilians-Universität München (LMU), Butenandtstraße 5-13, D-81377 München, Germany
[b] Bruker BioSpin GmbH, Silberstreifen, 76287 Rheinstetten, Germany

ARTICLE INFO

Article history:
Received 13 May 2009
Revised 16 July 2009
Available online 19 July 2009

Keywords:
Quantification
Phase error
Solid-state NMR
Quantitative NMR
MAS
Lineshape
Phase

ABSTRACT

Accurate determination of ^{1}H NMR signal intensities is useful for quantitative analysis of the hydrogen content and also to determine the relative peak intensity ratios in different application scenarios. To this end we have investigated the reliability and sources of intensity errors in ^{1}H solid-state MAS NMR. If sufficient resolution can be achieved by very high spinning speeds and high magnetic fields, quantification is straight forward. However, for poorly resolved spectra we show that small phase errors add a considerable amount of uncertainty. An analytical expression for the phase induced intensity-errors allowed us to suggest a robust and reliable recipe which is based on a combination of the spin-echo experiment, an extrapolation technique and a deconvolution algorithm which includes fitting of the signal phase. It significantly reduces errors caused by phase distortions, homonuclear dipolar dephasing, the receiver dead time delay and baseline rolling. The method was validated experimentally on samples with strong homonuclear dipolar interactions.

1. Introduction

One of the attractive features of NMR is that signals are proportional to the number of detected spins, which allows to perform quantitative analysis by NMR (qNMR). Unlike ordinary chemical analysis by other chemical or physical methods NMR not only allows to determine the total amount of an NMR active isotope but also its amount in different chemical environments.

Since qNMR is well established in liquid-state NMR [1,2] here we focus on quantification of solid-state NMR spectra. Under typical conditions the sensitivity of the NMR experiment is rather limited which does not make NMR a likely candidate for trace analysis where the analyte is below 1% in concentration. Applications of solid-state qNMR are wide spread too, covering different areas as, for example pharmaceutical formulation [3,4], cement base materials [5,6], drugs [7–9], coals [10] or amorphous materials [11] and different nuclei like ^{13}C [3,9,12–14], ^{29}Si [13], ^{119}Sn [13] and ^{23}Na [15]. Interestingly methods based on ^{13}C-CP-MAS NMR have proved to be quantifiable for organic matter [13].

A particularly tempting target/analyte for quantification are hydrogen atoms. In solids the hydrogen content is usually quantified by combustion analysis [16] which gives reliable results in many cases. However, ^{1}H solid-state NMR is a very sensitive probe and the resolution has improved significantly even in single-pulse excitation (SPE) experiments with the advent of very fast magic-angle-spinning probes [17]. Moreover, ^{1}H qNMR allows to distinguish between chemically relevant hydrogen and hydrogen coming from impurities (e.g. laboratory grease) and works even in cases where simple combustion analysis fails because of the stability of the samples as in case of ceramics or some inorganic solids. ^{1}H qNMR even complements X-ray diffraction because NH and O fragments can hardly be distinguished from one another in the diffraction pattern, while hydrogen in hydrogen-bonds often results in exceptional chemical shift values (10–18 ppm [18–21]) which helps spectral resolution and assignment in the NMR spectrum.

Systematic studies in solid-state qNMR have highlighted different sources of errors, for example repetition delays (related to spin–lattice relaxation) [3,9], pulse-length effects [9], spectrometer stability issues [15], sample preparation, quantitative analysis with internal or external reference [2,3,14,15] and packing effects of the material in the MAS rotor [14,15], which lead to false intensities when excited by inhomogeneous radio-frequency fields. An exhaustive protocol for solid-state qNMR has recently been published [9].

As for other analytical methods also in qNMR many of the above mentioned problems can be circumvented by quantification relative to an internal reference [2,3], in contrast to quantification to an external reference, which critically depends on the stability of the spectrometer sensitivity constant. For this purpose the to-be-analyzed sample is mixed with a known reference sample of high purity (internal reference) where the mass ratio, reference

* Corresponding author. Fax: +49 89 2180 77440.
E-mail address: gunnej@cup.uni-muenchen.de (J. Schmedt auf der Günne).

1090-7807/$ - see front matter © 2009 Elsevier Inc. All rights reserved.
doi:10.1016/j.jmr.2009.07.019

mass m_{ref} to analyzed sample mass m_{sample}, is known. The area below a peak a is proportional to the number of nuclei detected by NMR. Consequently, the ratio of peak areas is proportional to the ratio of the number of detected nuclei n_{nuc} in mole in the analyte and the reference sample in the ideal case. Because the molar mass and the number of detected nuclei per mole x_{ref} of the reference sample is known, the ratio $\frac{n_{nuc,analyte}}{n_{nuc,ref}}$ may be rewritten in the following form.

$$\frac{a_{analyte}}{a_{ref}} = \frac{n_{nuc,analyte}}{n_{nuc,ref}} = \frac{n_{nuc,analyte}}{n_{ref}x_{ref}} = \frac{n_{nuc,analyte}}{m_{ref}/M_{ref}x_{ref}} \tag{1}$$

Variations in natural abundance of the detected isotope have been neglected for simplicity. The result of a quantification is typically given in mole analyte per mass $\frac{n_{nuc,analyte}}{m_{sample}}$. Its calculation from Eq. (1) is straight forward. In our experience the usage of an internal reference improves the relative error of $\frac{n_{nuc,analyte}}{m_{sample}}$ from about 30% for quantification to an external reference to below 10% for spin-1/2 nuclei other than ^{19}F and ^{1}H (results not shown).

Because our first results of solid-state ^{1}H qNMR on amorphous samples were disappointing, here we present an analysis of possible errors and an improved protocol. Our hypothesis is that the combination of receiver dead time delay, homonuclear dipolar dephasing and baseline distortions leads to frequency dependent phase shifts of the signal which cause significant errors in qNMR with internal references. To test the hypothesis we derive an analytical expression for the relative error of the peak area ratio of two dephased peaks of Lorentzian lineshape. We then propose a protocol based on an extrapolation approach and the Hahn echo [22] which avoids the receiver dead time and accounts for intensity losses through homonuclear dipolar dephasing and transversal relaxation. Finally, the protocol is validated for a sample with strong ^{1}H–^{1}H magnetic dipole–dipole couplings at low magnetic fields and moderate sample spinning frequencies and compared to data obtained at medium magnetic fields and very high sample spinning frequencies.

2. Theory

The hypothesis of this contribution is that even when following the protocol presented in Ref. [9,14] phase errors may distort the lineshape of a neighboring peak to such an extent that in case of broad, poorly resolved peaks a significant error in the determined peak area ratio may result. A visual presentation of the idea is presented in Fig. 1. A small phase error will cause an admixture of dispersive lineshape of peak A to peak B so that amplitude of peak B is virtually decreased while in reverse peak B adds a bit of intensity to peak A. We conclude that the resulting error in peak ratio r depends on the signal phase ϕ and may be positive or negative. Because dispersive lineshapes have a much slower decaying behavior away from the center frequency than their absorptive counterparts, it is interesting to ask in which cases this mechanism is relevant. In the following we derive an estimate of this error based on Lorentzian lineshapes.

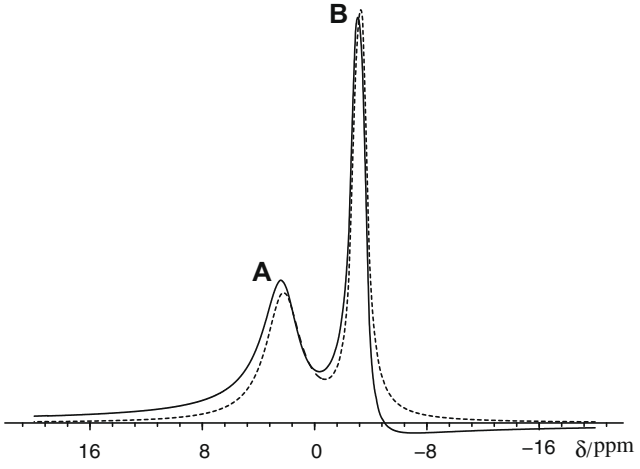

Fig. 1. Simulated NMR spectra of a line shape function perfectly in phase (dotted line) and a lineshape being out of phase (signal phase ϕ = 10°) but with otherwise identical lineshape parameters.

To derive a simple analytical expression of the relative error $\frac{\Delta r}{r}$ of the peak ratio r which results from a dephased spectrum of two peak A and B, we need to make a number of simplifying assumptions. We assume the two peaks can be described as Lorentzian functions with the parameters integrated peak area a, linewidth (full width at half height in Hz) λ_i and center frequency ν_i for peak i. The real part of complex Lorentzian [23] $L_i(\nu,\nu_i,\lambda_i,a_i,\phi)$ may be written in terms of an absorptive $L_{abs,i}(\nu,\nu_i,\lambda_i)$ and a dispersive contribution $L_{dis,i}(\nu,\nu_i,\lambda_i)$.

$$\begin{aligned} L_{abs,i}(\nu,\nu_i,\lambda_i) &= \frac{\lambda_i/2}{\pi((\lambda_i/2)^2+(\nu-\nu_i)^2)} \\ L_{dip,i}(\nu,\nu_i,\lambda_i) &= \frac{-(\nu-\nu_i)}{\pi((\lambda_i/2)^2+(\nu-\nu_i)^2)} \end{aligned} \tag{2}$$

The spectral lineshape of a resonance with a phase ϕ can be determined by evaluating the following function over all frequencies ν. A peak in pure absorption then has a phase of 0°.

$$L_i(\nu,\nu_i,\lambda_i,a_i,\phi) = a_i(\cos(\phi)L_{abs,i}(\nu,\nu_i,\lambda_i) - \sin(\phi)L_{dis,i}(\nu,\nu_i,\lambda_i)) \tag{3}$$

The total lineshape $S_{\exp}(\nu)$ of a dephased spectrum consisting of two peaks can be written as follows.

$$S_{\exp}(\nu) = L_A(\nu,\nu_A,\lambda_A,a_A,\phi) + L_B(\nu,\nu_B,\lambda_B,a_B,\phi) \tag{4}$$

In order to deconvolute such a spectrum we assume it is being fitted with two Lorentzian lineshapes in pure absorption, i.e. $\phi = 0$, where linewidths and center frequencies do not change.

$$S_{fit}(\nu) = L_{abs,A}(\nu,\nu_A,\lambda_A,a_{Afit}) + L_{abs,B}(\nu,\nu_B,\lambda_B,a_{Bfit}) \tag{5}$$

The task is to find the fitted peak areas a_{Afit}, a_{Bfit} which give the smallest deviation between $S_{fit}(\nu)$ and $S_{\exp}(\nu)$ in other words the smallest "total square error" E.

$$E = \int_{-\infty}^{+\infty} (S_{\exp} - S_{fit})^2 d\nu \tag{6}$$

Necessary conditions for the optimum set of parameters a_{Afit}, a_{Bfit} are

$$\frac{\partial E}{\partial a_{Afit}} = 0 \ \wedge \ \frac{\partial E}{\partial a_{Bfit}} = 0 \tag{7}$$

These two equations can be solved simultaneously for a_{Afit} and a_{Bfit}, the term $\nu_A - \nu_B$ is substituted by $\Delta\nu$, the sum of linewidths $\lambda_A + \lambda_B$ by λ_s, the term a_A/a_B by r and the relative error $\frac{\Delta r}{r} = \frac{a_{Afit}/a_{Bfit} - a_A/a_B}{a_A/a_B}$ of the ratio is calculated in Eq. (8). Because experimental spectra are usually "phased" such that the phase ϕ is very close to zero a Taylor expansion up to second order of ϕ around 0° may be applied to identify the main sources of error.

$$\frac{\Delta r}{r} \approx X_1 \cdot \phi + X_2 \cdot \phi^2 \tag{8}$$

where X_1 and X_2 (see Supporting information) are

$$X_1 = \frac{4\lambda_s(\lambda_A\lambda_s + 4\lambda_A\lambda_B r + \lambda_B\lambda_s r^2)\Delta\nu + 16(\lambda_A + \lambda_B r^2)\Delta\nu^3}{r((\lambda_A^2 - \lambda_B^2)^2 + 8\lambda_s^2\Delta\nu^2 + 16\Delta\nu^4)} \tag{9}$$

This formula provides an error estimate for a given set of line shape parameters of two peaks. We calculated plots of the relative error $\Delta r/r$ as a function of the signal phase ϕ for a particular intensity ra-

tio r (see Fig. 6) and as a function of the peak area ratio r at a particular phase ϕ (see Fig. 7) by using the formula in Eq. (8). From the curves it is clear that not only the signal phase has a significant influence when its values deviate from 0° but also that relative error passes through a minimum which is located at a peak area ratio r close to 1. It should be noted that these formulas only apply to the case of pure Lorentzian lineshapes and not to lineshape functions like Gaussian or Voigt functions. The latter have a faster decaying characteristic away from the lineshape center, therefore above a certain minimum peak difference the given error should serve as an upper limit of the peak area ratio.

We conclude that uncertainties in the signal phase may become the main source of error (see Section 4) if spectra are only poorly resolved as in case of the slow-spinning spectrum in Fig. 2. While qualitatively this has been noted before [24,25], we provide an error estimate based on a simple analytical formula.

How can the phase induced error be reduced? Usually during phase correction of a spectrum (called "phasing") the operator manually or automatically [26–29] applies a phase shift ϕ to each point of the spectrum [23]. The phase ϕ is often chosen to be a linear frequency dependent function. If the frequency dependent component (first-order correction) is absent then the phase shift can be described by a constant ϕ_0 (zeroth-order correction) which is applied to all data points in the spectrum. The frequency dependent contribution is necessary to compensate for phase shifts caused by the receiver dead time delay in SPE experiments, finite pulse effects and bandwidth limitations of the spectrometer. After phase correction the frequency dependent contribution manifests itself in form of a rolling baseline in the spectrum ([30], p. 145) which is then removed by subtraction of a calculated baseline function. Critical steps in this procedure are the manual phase correction which will automatically cause instabilities in the phase ϕ and the baseline correction. Baseline correction however is difficult in poorly resolved spectra because not enough true baseline points are available. In our opinion baseline corrections are especially critical and should be avoided for the given reasons. Baseline distortions can significantly be reduced by avoiding the receiver dead time delay with the help of a rotor-synchronized spin-echo sequence (see Fig. 3). The recipe presented below is therefore based on quantification with the Hahn spin-echo, combined with automatic phasing which is included in the deconvolution process. Like that manual interference by the operator is avoided and the resulting intensity errors are reduced. However, due to longer delays before the acquisition intensity losses by finite pulse effects, transversal relaxation and dipolar dephasing need special consideration (see below).

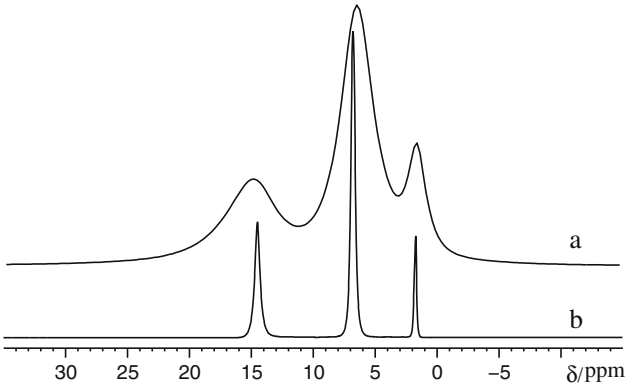

Fig. 2. ^{1}H MAS NMR spectra of a mixture of adamantane and ammonium dihydrogenphosphate obtained at (bottom to top) 65 and 25 kHz sample spinning speed, respectively; spectrum (b) was recorded at 600 MHz and spectrum (a) was recorded at 200 MHz resonance frequency.

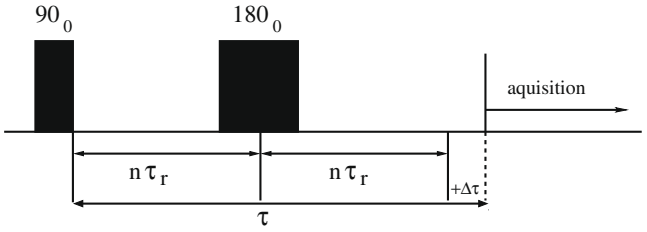

Fig. 3. Modified rotor-synchronized spin-echo pulse sequence used for quantitative measurements; τ_r designates a rotor period, $\Delta\tau$ is a small delay which has to be determined once so that (small) first-order phase corrections become unnecessary; these are caused by finite pulse effects and hidden delays in the receiver of the NMR spectrometer.

3. Results and discussion

3.1. Quantification protocol

The following protocol is an incomplete [9,14] listing of steps necessary for ^{1}H NMR quantification to compensate for the sources of intensity ratio errors as explained above. For spectrometer settings, signal-to-noise ratios, setting of repetition delays [24] and various details of qNMR experiments consult Refs. [9,14].

1. Choose internal reference. The reference should be chemically inert and its peak(s) must be distinguishable from sample peaks.
2. Weigh in internal reference and to-be-analyzed sample. If possible choose the mass ratio such that peak areas of analyte and internal reference are of similar size.
3. Make a homogeneous mixture.
4. Obtain quantitative MAS NMR spectra at highest available magnetic field and sample spinning frequencies. Choose spectrometer settings which make first-order phase corrections and consequently baseline corrections of the spectrum unnecessary. Use a rotor-synchronized Hahn echo and acquire spectra at different τ values (see Fig. 4). Subtract the probe ^{1}H background if necessary.

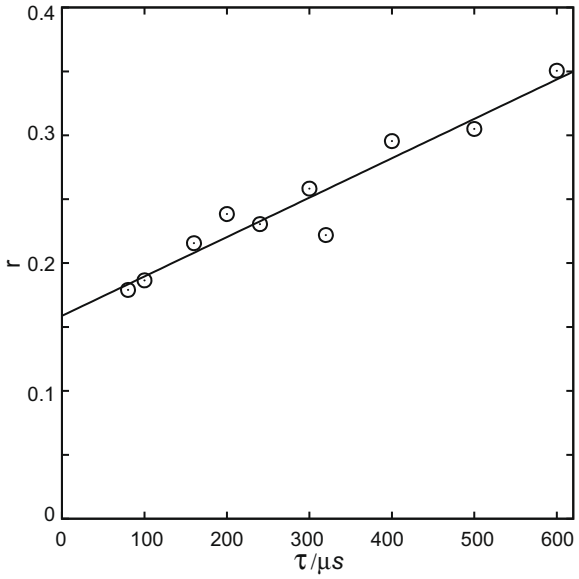

Fig. 4. Experimental peak area ratio as a function of the spin-echo delay τ (see Fig. 3) for a mixture of adamantane and ammonium dihydrogenphosphate (mixture 5, see Table 1) determined by ^{1}H MAS NMR; the solid line was obtained by linear regression; experimental conditions (case III, see text): sample spinning speed ~25 kHz, magnetic field of 4.7 T.

5. Determine peak area ratios $a_{analyte}/a_{ref}$ by deconvolution of spectra. Set lineshape parameters on pure samples separately. Use constrained fitting with more than one set of Gauss/Lorentzian lineshape parameters per peak if necessary. Zeroth-order spectral phase should be fitted simultaneously.
6. Extrapolate the peak area ratio $a_{analyte}/a_{ref}$ to τ equals zero, if the spin-echo experiment was used to acquire quantitative spectra.
7. Calculate analyte per mass ratio with Eqs. (10) and (11), so that offset dependent pulse excitation effects are considered.

$$\frac{f(r_{off,ref})}{f(r_{off,analyte})}\frac{a_{analyte}}{a_{ref}}=\frac{n_{nuc,analyte}}{m_{ref}/M_{ref}x_{ref}} \tag{10}$$

In the following we will explain which considerations lead to the individual points in the protocol.

To 1: The choice of an appropriate internal reference next to the mentioned criteria should be based on short spin–lattice relaxation times, sharp resonances.

To 2: This step generally represents the smallest source of error if properly handled. For hygroscopic or air-sensitive samples a glove box filled with Ar or N_2 as inert gas may be beneficial. A peak area ratio close to 1 helps reducing errors from small errors in the phase correction.

To 3: Making the sample homogeneous can be difficult, if as in the case of adamantane one of the components has a tendency to stick to tools like the agate mortar. Sample losses can in principle be estimated by preparing a series of mixtures with different ratios, which should give the same results.

To 4: If resonances are properly resolved no special precautions have to be taken and simple single-pulse excitation is the method of choice. Then however proper baseline correction will be necessary. If the spin-echo experiment is used, first-order phase correction and hence baseline correction will not be necessary. In principle it should be possible to use composite pulses to increase the bandwidth of the spin-echo experiment, however we require not only broadband excitation with respect to the magnitude of the signal but also no phase distortions. For this reason we use the ordinary spin-echo experiment as indicated in Fig. 3 which has the advantage of an almost perfectly linear phase profile at the cost of a reduced excitation bandwidth as compared with single-pulse excitation (see Fig. 5). We modified the original spin-echo experiment by a small delay $\Delta\tau$ to compensate linear phase errors caused by finite and hidden delays in the receiver within the experiment.

The intensity of spinning sidebands should be reduced as much as possible by high sample spinning frequencies to increase resolution, to increase signal-to-noise ratio, to reduce dipolar dephasing during the spin-echo experiment and because the handling of off-resonance effects is simplified. High magnetic fields can help to increase resolution because line broadening through zeroth-order rotational resonance is reduced.

To 5: Because integration as a means to determine peak areas is not feasible if resonances are not well resolved deconvolution has to be used. Deconvolution of spectra of solid samples is generally not simple and complicated lineshapes might require constrained deconvolution with several Gauss–Lorentzian functions per peak. Especially when spectra with extreme intensity ratios are deconvoluted it is advisable to "train" the lineshape deconvolution program on the pure samples because tiny deviations in the main peak will distort the lineshape of the weaker peaks significantly. In order to reduce errors by an incorrectly chosen phase ϕ_0 the final step in the lineshape fitting procedure should include the phase ϕ_0 and the peak areas in the list of variable parameters.

To 6: During the evolution period τ (see Fig. 3) strong magnetic homonuclear dipole–dipole interactions between hydrogen nuclei and transversal relaxation will cause a decay of the magnetization. The former is a coherent process, we refer to as "dipolar dephasing". If several rotor-synchronized spin-echo experiments have been recorded with variable delays τ then it is possible to extrapolate the peak intensities/areas to zero delay, so that the peak area ratios are virtually freed of errors caused by dipolar dephasing and transversal relaxation.

To 7: If the sample is spun fast enough, so that no spinning sidebands are visible, then the off-resonance losses can be quantified and corrected for with simple analytical formulas for signal magnitude, otherwise losses can be accessed by numerical programs only. The signal yield $f(r_{off})$ in the spin-echo experiment is a simple function independent from the delay τ, if transversal relaxation and dipolar dephasing are neglected.

$$f(r_{off})=\frac{|a(r_{off})|}{|a(0)|}=\frac{\sqrt{2}\sqrt{1+2r_{off}^2+\cos\left(\frac{1}{2}\pi\sqrt{1+r_{off}^2}\right)}\cdot\sqrt{\sin\left(\frac{1}{4}\pi\sqrt{1+r_{off}^2}\right)^2}\cdot\sin^2\left(\frac{1}{2}\pi\sqrt{1+r_{off}^2}\right)}{\left(1+r_{off}^2\right)^2} \tag{11}$$

where $r_{off}=\frac{\nu_{offset}}{\nu_{rf}}$ and $|a(0)|$ is the integrated peak area measured on resonance.

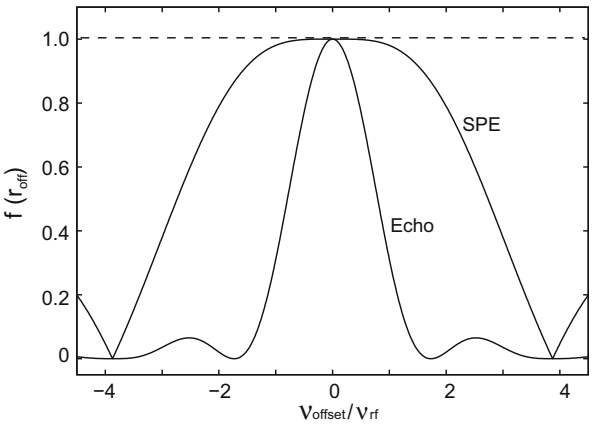

Fig. 5. Signal yield as a function of the offset factor ν_{off}/ν_{rf} of a single-pulse excitation experiment (SPE with a pulse with 90° flip angle) and a spin-echo experiment (Echo); ν_{off} is the difference between transmitter frequency and Lamor frequency, ν_{rf} is the pulse nutation frequency ν_{rf} (see text).

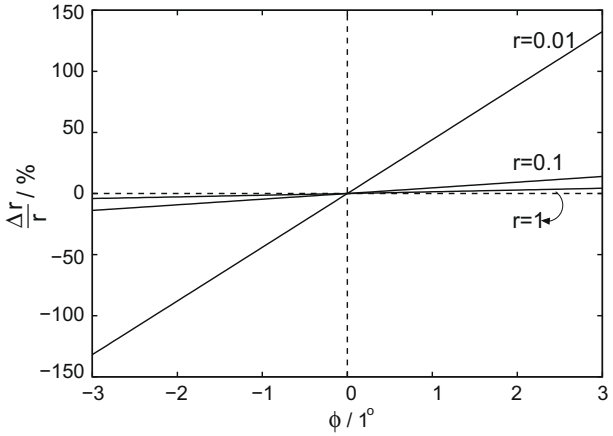

Fig. 6. Relative error of the peak area ratio $\frac{\Delta r}{r}$ as a function of the signal phase ϕ for a given peak area ratio r; the curves were calculated by using the analytical expression presented in Eq. (8); the lineshape parameters refer to peaks of adamantane and ammonium dihydrogenphosphate as specified in the text $\lambda_{\text{adamantane}}=290.0$ Hz; $\lambda_{\text{ammonium dihydrogenphosphate}}=530.0$ Hz and $\Delta\nu=1008.0$ Hz.

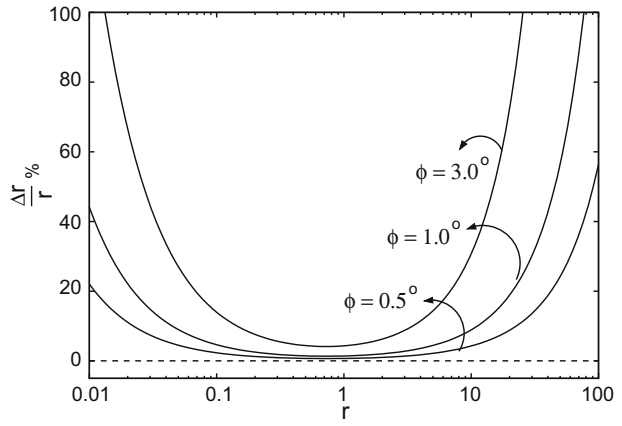

Fig. 7. Relative error of the peak area ratio $\frac{\Delta r}{r}$ as a function of peak area ratio r for a given signal phase error ϕ; the curves were calculated by using the analytical expression presented in Eq. (8); the used lineshape parameters refer to peaks of adamantane and ammonium dihydrogenphosphate as specified in the text $\lambda_{\text{adamantane}} = 290.0$ Hz; $\lambda_{\text{ammonium dihydrogenphosphate}} = 530.0$ Hz and $\Delta\nu = 1008.0$ Hz.

This formula has been obtained by explicit calculation of the evolution of the spin density matrix in the spin-echo experiment under consideration of a transmitter frequency offset ν_{offset} and spin-echo pulses with a nutation frequency ν_{rf}, which is defined as the inverse of the length of a pulse with 360° flip angle.

4. Validation

Will the phase error cause a relevant error under typical experimental conditions? As an example we have calculated the estimated errors for the two ^{1}H NMR spectra for a mixture of adamantane and ammonium dihydrogenphosphate in Fig. 2. The peak parameters were chosen from a deconvolution with pure Lorentzian functions and a typical error of the signal phase was estimated from the standard deviation for the zeroth-order phase when processing the data manually several times. Since ammonium dihydrogenphosphate has two different resonances at 6.4 and 14.9 ppm, we have chosen only the one peak which is closer to the adamantane resonance for the calculation of the phase induced error. The calculated relative error $\Delta r/r$ by using Eq. (8) at a sample spinning speed of 25 kHz was 5.5% (standard deviation of the zeroth-order phase 2.93°), while the relative error for a spin-echo experiment at a sample spinning frequency of 65 kHz was only 0.08% (standard deviation of the zeroth-order phase 0.2°). Clearly for spectra with low resolution as the one presented at 25 kHz sample spinning frequency the phase error presents a significant source of error.

Next we wish to provide proof for an improvement in the quality of quantification by applying the presented protocol based on the spin-echo experiment, deconvolution including phase fitting and extrapolation to zero τ delays. To this end we have prepared a series of mixtures of adamantane and ammonium dihydrogenphosphate with different but known mass ratio as reported in Table 1. Adamantane was chosen because is well suited to act as an internal standard for quantitative ^{1}H NMR analysis. Ammonium dihydrogenphosphate is an example for a sample with strong dipolar couplings which cause significant line broadenings.

For comparison we have determined peak areas by deconvolution from experimental spectra of the specified mixtures under different conditions. In all cases the spectra were acquired with sufficiently long repetition delays and the same samples were used. To mimic low-resolution conditions we acquired spectra by single-pulse excitation, at low magnetic field (4.7 T) and at only 25 kHz sample spinning frequency (case I). For high-resolution conditions we chose a magnetic field of 14.1 T, a sample spinning frequency of 65 kHz and the spin-echo experiment (case II). Finally, we applied the presented recipe (case III) under the low-resolution conditions of case I. The results are shown in Fig. 8 in the form of correlation plot where the observed peak area ratio r_{obs} is shown as a function of the ratio r_{exp}, which is expected by composition. The estimated standard deviations of the relative error for case I, case II and case III are 62%, 4.1% and 4.9%, respectively. The results indicate that even under low-resolution conditions reliable quantification can be achieved if the presented protocol is being followed. The peak area ratios of the analyte and the internal reference in this study cover a range of approximately from 4:5 to 12:1 and all give satisfactory results. It is remarkable that the curve for case I (see Fig. 8) shows a systematic error to higher peak area ratios, which has been abolished completely by the use of the suggested protocol (case III).

Note that in case III we also applied the suggested extrapolation to zero τ values. In Fig. 4 the peak area ratios of a particular mixture are plotted against the spin-echo delay τ. The τ values were modified by using integer multiples of the rotor period for $\tau/2$ and/or choosing slightly different spinning frequencies in the spin-echo experiment. In our example, extrapolation to zero τ values may be achieved by linear regression. As compared to a τ value of 80 μs the true peak area ratio is only 86% of the former. Because the term $\frac{f(r_{off,ref})}{f(r_{off,analyte})}$ does not depend on the ratio of the mixture, the same correction term has been applied to all determined peak area ratios r_{obs}.

To which extent do the various described mechanisms contribute to the error of the peak area ratio? Fig. 4 indicates that losses through relaxation and dipolar dephasing are negligible in case I while in case III the error amounts to 14%. From the given formulas it is clear that off-resonance effects are negligible in the presented cases (i.e. <0.5%). Errors through the manual setting of the spectral phase (zeroth-order "phasing") amount to 5.5%, 0.08% in case I and case II, respectively (see above). In single-pulse excitation experiments it is difficult to disentangle errors caused by baseline rolling, baseline corrections and signal phase. However, from the difference between the estimated standard deviations in case I of 62% and the above mentioned sources of errors we conclude that it could amount up to 42%. We conclude that in the presented low-field case measures to reduce baseline distortions (and therefore the need for first-order phasing) have the biggest influence on the relative peak ratio error, followed by losses through relaxation/dipolar dephasing, followed by errors through the manual setting of the spectral phase and last by finite pulse errors.

5. Experimental

The samples adamantane $C_{10}H_{16}$ (ACROS Organics, 99%) and ammonium dihydrogenphosphate $NH_4H_2PO_4$ (Grüssing >99%) were used without any further purification. Different mixtures were prepared by adding the two compounds in an appropriate

Table 1
Sample mixtures of adamantane and ammonium dihydrogenphosphate used in Fig. 8 and the expected peak area ratio r_{exp} defined as $a(NH_4H_2PO_4)/a(C_{10}H_{16})$.

Mixture	$m(C_{10}H_{16})$/mg	$m(NH_4H_2PO_4)$/mg	r_{exp}
1	1012.3	2055.9	1.11
2	512.0	420.7	2.74
3	100.0	550.6	0.41
4	621.1	620.3	2.25
5	62.8	1062.4	0.13
6	199.6	450.3	0.99
7	454.8	87.6	11.70
8	450.0	150.0	6.76

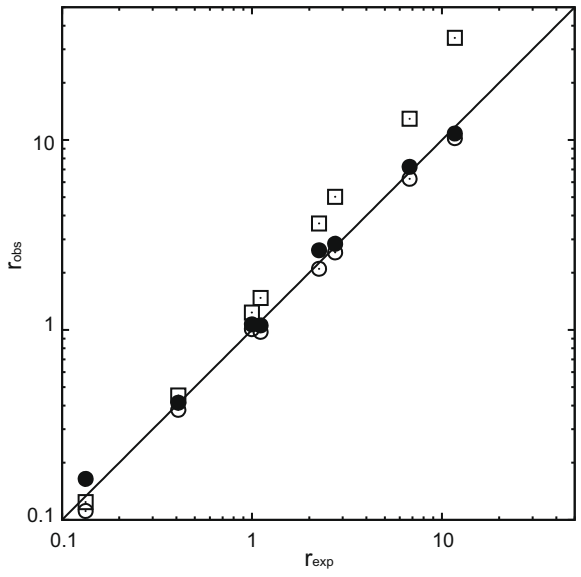

Fig. 8. Observed peak area ratio r_{obs} as a function of peak area ratio r_{exp} expected from composition of the adamantane/ammonium dihydrogenphosphate mixture (see Table 1) by ^{1}H MAS NMR; filled circles and squares denote data from spin-echo and SPE experiments at a sample spinning speed of 25 kHz recorded at a magnetic field of 4.7 T, respectively (case I and III, see text); empty circles are data from spin-echo experiments at a sample spinning frequency of 65 kHz recorded at a magnetic field of 14.1 T (case II); repeated analysis was performed for individual data points including the full protocol from weighing of the samples to a deconvolution of the peak intensities; the observed standard deviations ($r = 1.11$, case I: 7%, case II: 6%) are in line with the scatter of the data points observed above.

composition (see Table 1). Samples were made homogeneous by finely grinding the mixtures with the help of an agate mortar.

Solid-state NMR experiments were conducted at a magnetic field of 4.7 T on a Bruker AvanceII-200 equipped with a 2.5-mm double resonance MAS probe at ^{1}H frequency of 200.175 MHz and at a magnetic field of 14.1 T on a Bruker AvanceIII-600 spectrometer equipped with a 1.3-mm triple resonance MAS probe at ^{1}H frequency of 600.13 MHz. The one-dimensional (1D) ^{1}H NMR spectrum was acquired with a 90° pulse length of 2.5 μs, recycle delays of 16 s and at sample spinning frequency of 25 kHz, while spectra at 65 kHz were collected using excitation pulses of 2 μs, and recycle delays of 8 s. The spin-echo sequence selected coherence transfer pathways with a 16 step phase cycle. The repetition delay was chosen to ensure negligible intensity errors by insufficient longitudinal relaxation, i.e. longer than $5 \cdot T_1$. In order to reduce spectrometer bandwidths distortions from the digital filters we chose the biggest spectral widths possible.

6. Conclusion

We have shown how ^{1}H NMR needs to be used in order to quantify the hydrogen content in solid materials. The basic idea is that the signal phase is becoming an important source of error once the spectral resolution decreases below a certain limit. In that case the usual method – single-pulse excitation followed by baseline correction and deconvolution – fails. The presented equations give an estimate for the phase error for a given set of lineshape parameters and help with the decision whether phase errors need to be considered or not. An important conclusion drawn from the presented formula is that extreme intensity ratios between the peaks of the internal reference and the analyte are to be avoided. If phase errors need to be considered, we have shown that an experimental protocol including the spin-echo experiment, an extrapolation technique and phase fitting may reestablish error margins similar to those under high-resolution conditions. High-resolution conditions may sometimes be achieved simply by doing the experiments in high magnetic fields combined with the highest currently available magic-angle sample spinning frequencies. We believe that the presented approach can be transferred to other nuclei like, for example ^{19}F. It is not only of relevance for qNMR in the sense of an absolute quantification of hydrogen content in a sample but also for quantifying relative peak intensities which is useful for locating hydrogen atoms in crystalline solids.

Acknowledgments

J.S.a.d.G. and Y.S.A. gratefully acknowledge financial support through the Emmy-Noether program of the DFG (SCHM1570-2) and the "Ludwig-Maximilians-Universität". We are also grateful to Prof. Dr. W. Schnick for the possibility to use the facilities at the chair of inorganic solid-state chemistry, Dr. J. Weber for fruitful discussions, Dr. H. Förster for technical advice and C. Minke for technical support.

Appendix A. Supplementary data

Supplementary data associated with this article can be found, in the online version, at doi:10.1016/j.jmr.2009.07.019.

References

[1] V. Rizzo, V. Pinciroli, J. Pharm. Biomed. Anal. 38 (2005) 851.
[2] S. Bekiroglu, O. Myrberg, K. Östman, M. Ek, T. Arvidsson, T. Rundlöf, B. Hakkarainen, J. Pharm. Biomed. Anal. 47 (2008) 958.
[3] R. Suryanarayanan, T.S. Wiedmann, Pharm. Res. 7 (1990) 184.
[4] B.N. Nelson, L.J. Shieber, D.H. Barich, J.W. Lubach, T.J. Offerdahl, D.L. Lewis, J.P. Heinrich, E.J. Munson, Solid State Nucl. Magn. Reson. 29 (2006) 204.
[5] J. Skibsted, S. Rasmussen, D. Herfort, H.J. Jakobsen, Cem. Concr. Comp. 25 (2003) 823.
[6] H. Hilbig, F.H. Kohler, P. Schiel, Cem. Concr. Res. 36 (2006) 326.
[7] T.J. Offerdahl, J.S. Salsbury, Z. Dong, D. Grant, S.A. Schroeder, I. Prakash, E.M. Gorman, D.H. Barich, E.J. Munson, J. Pharm. Sci. 94 (2005) 2591.
[8] I. Wawer, M. Pisklak, Z. Chilmonczyk, J. Pharm. Biomed. Anal. 38 (2005) 865.
[9] R.K. Harris, P. Hodgkinson, T. Larsson, A. Muruganatham, J. Pharm. Biomed. Anal. 38 (2005) 858.
[10] A. Jurkiewicz, G.E. Macie, Anal. Chem. 67 (1995) 2188.
[11] J. Schmedt auf der Günne, J. Beck, W. Hoffbauer, P. Krieger-Beck, Chem. Eur. J. 11 (2005) 4429.
[12] D.E. Bugay, Adv. Drug Deliv. Rev. 48 (2001) 43.
[13] R.K. Harris, Analyst 110 (1985) 649.
[14] S. Sanchez, F. Ziarelli, S. Viel, C. Delaurent, S. Caldarelli, J. Pharm. Biomed. Anal. 47 (2008) 683.
[15] F. Ziarelli, S. Viel, S. Sanchez, D. Cross, S. Caldarelli, J. Magn. Reson. 188 (2007) 260.
[16] K. Cammann, Instrumentelle Analytische Chemie, Spektrum, Akad. Verl., Heidelberg, 2001.
[17] A. Samoson, T. Tuherm, Z. Gan, Solid State Nucl. Magn. Reson. 20 (2001) 130.
[18] J.P. Yesinowski, H. Eckert, G.R. Rossman, J. Am. Chem. Soc. 110 (1988) 1367.
[19] A. Nag, B. Lotsch, J. Schmedt auf der Günne, O. Oeckler, P.J. Schmidt, W. Schnick, Chem. Eur. J. 13 (2007) 3512.
[20] M.A. Neelakantan, S. Thalamuthu, B.M. Drašković, G. Bogdanović, A.C. Chamayou, S. Banerjee, Y.S. Avadhut, J. Schmedt auf der Günne, C. Janiak, in preparation.
[21] E. Brunner, U. Sternberg, J. Prog. Nucl. Magn. Reson. 32 (1998) 21.
[22] E.L. Hahn, Phys. Rev. 80 (1950) 580.
[23] M.H. Levitt, Spin Dynamics, first ed., John Wiley and Sons, Ltd, New York, 2001.
[24] A.I. Popov, K. Hallenga, Modern NMR Techniques and Their Application in Chemistry, Practical Spectroscopy Series, 11, New York, 1991.
[25] C.H. Sotak, C.L. Dumoulin, G.C. Levy, in: G.C. Levy (Ed.), Topics in Carbon-13 NMR Spectroscopy, vol. 4, Wiley, New York, 1984, p. 91.
[26] R.R. Ernst, J. Magn. Reson. 1 (1969) 7.
[27] J.M. Daubenfeld, J.C. Boubel, J.J. Delpuech, J. Magn. Reson. 195 (1985) 62.
[28] D.E. Brown, T.W. Campbell, R.N. Moore, J. Magn. Reson. 85 (1989) 15.
[29] F. Montigny, K. Elbayed, J. Brondeau, D. Canet, Anal. Chem. 62 (1990) 864.
[30] K. Schmidt-Rohr, H.W. Spiess, Multidimensional Solid-State NMR and Polymers, Academic Press, New York, 1999.